

Supramolecular Materials with Electroactive Chemical Functions**

Gregory N. Tew, Martin U. Pralle, and Samuel I. Stupp*

Discovering and understanding the important forces in molecular self-assembly continues to be an area of great interest in materials science. Many groups are working in this field and perhaps just as many different strategies are employed to control the organization of molecules.^[1, 2] In recent years, our laboratory has reported on a class of supramolecular materials formed by molecules with triblock architecture, termed rodcoil molecules, that self-organize into discrete mushroom-shaped nanostructures. To date all systems studied consist of a diblock coil of oligostyrene and oligoisoprene or oligobutadiene covalently attached to a rigid block made up of biphenyls linked through ester bonds.^[3–5] A more recent report described a set of triblock molecules based on styrene and isoprene but rod segments containing phenylene vinylene (PV) sequences in addition to biphenyl esters.^[6, 7]

The study of these materials enabled us to gain an understanding of the important factors leading to the formation of nanostructured supramolecular materials.^[5, 7] One important factor in these systems is the architectural design, where a large, bulky amorphous coil is attached to a rigid, well-defined rod compound by a flexible, amorphous segment with smaller cross-section. Also, the diblock coil to rigid rod volume fraction was proposed to have a large impact on the ability of the systems to self-organize into discrete nanostructures. Perhaps the best test for these principles is the design of systems with very different chemistries that retain the architectural requirements of rodcoil **2** (see Scheme 2). The chemical structure shown in Scheme 2 as molecule **1** was chosen to test our hypothesis and the general applicability of the triblock architecture to order into discrete nanostructures. These molecules contain a diblock coil of oligo-4-diphenylaminostyryl-ethylene oxide and an oligomer of phenylene vinylene.

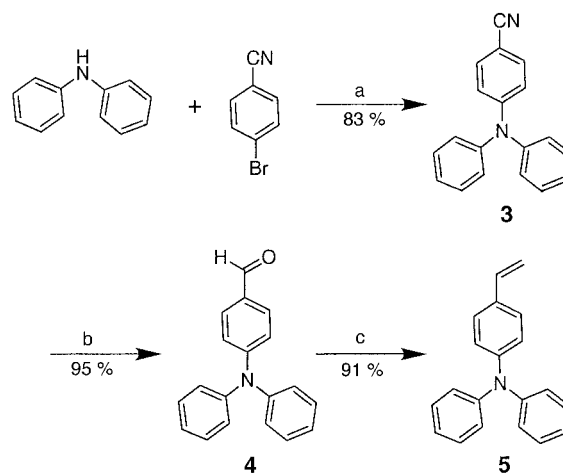
Triphenylamines (TPAs) are currently of interest as hole transport layers in light-emitting devices and are used extensively in the photocopying and laser-printing industry.^[8] Incorporating this functionality into the rodcoil architecture could potentially lead to unique nanostructured optoelectronic devices. This inspired the development of monomer **5** (see Scheme 1). In addition to these photonic properties, this segment must have a structure mimicking styrene within the

triblock architecture, where the block is amorphous and sterically larger than either of the other two blocks.

The second block of the coil is ethylene oxide and represents a drastic change in chemical properties from isoprene or butadiene but is architecturally very similar. Chemically, these dienes are highly diverse with roughly a 50:50 ratio of 1,4- and 1,2-addition products plus a great range of stereochemical diads along the backbone.^[9] By contrast, polymerized ethylene oxide does not produce any of these diversities. Furthermore, ethylene oxide is hydrophilic while the dienes are hydrophobic. Although ethylene oxide differs greatly in a chemical context from the dienes, architecturally they are quite similar because both have a very small cross-section and are highly flexible linear coils.

A rigid rod block of pentameric PV represents the third block of the triblock architecture in **1** and replaces the biphenyl segments found in the original triblock molecule **2**. Again, while PV is different chemically, it has the same architectural features as the biphenyl esters and provides similar driving forces for self-organization. Here we report the synthesis and characterization of supramolecular films composed of **1**.

Traditionally the synthesis of TPA derivatives involved exceedingly harsh conditions, generally leading to low yields for sensitive molecules.^[10] However, this situation changed greatly in the last few years due to seminal work by Hartwig^[11] and Buchwald et al.^[12] on the chemistry of aromatic aminations.^[13] Ligand choice was shown to greatly affect the yield of the reaction, and 1,1'-bis(diphenylphosphanyl)ferrocene (dppf) is best for synthesizing TPA derivatives.^[14] Aromatic amination using diphenylamine and 4-bromobenzonitrile produced **3** in 83 % yield (Scheme 1). The cyano group was then reduced and the product **4** under Wittig-type conditions transformed to **5**.^[15]

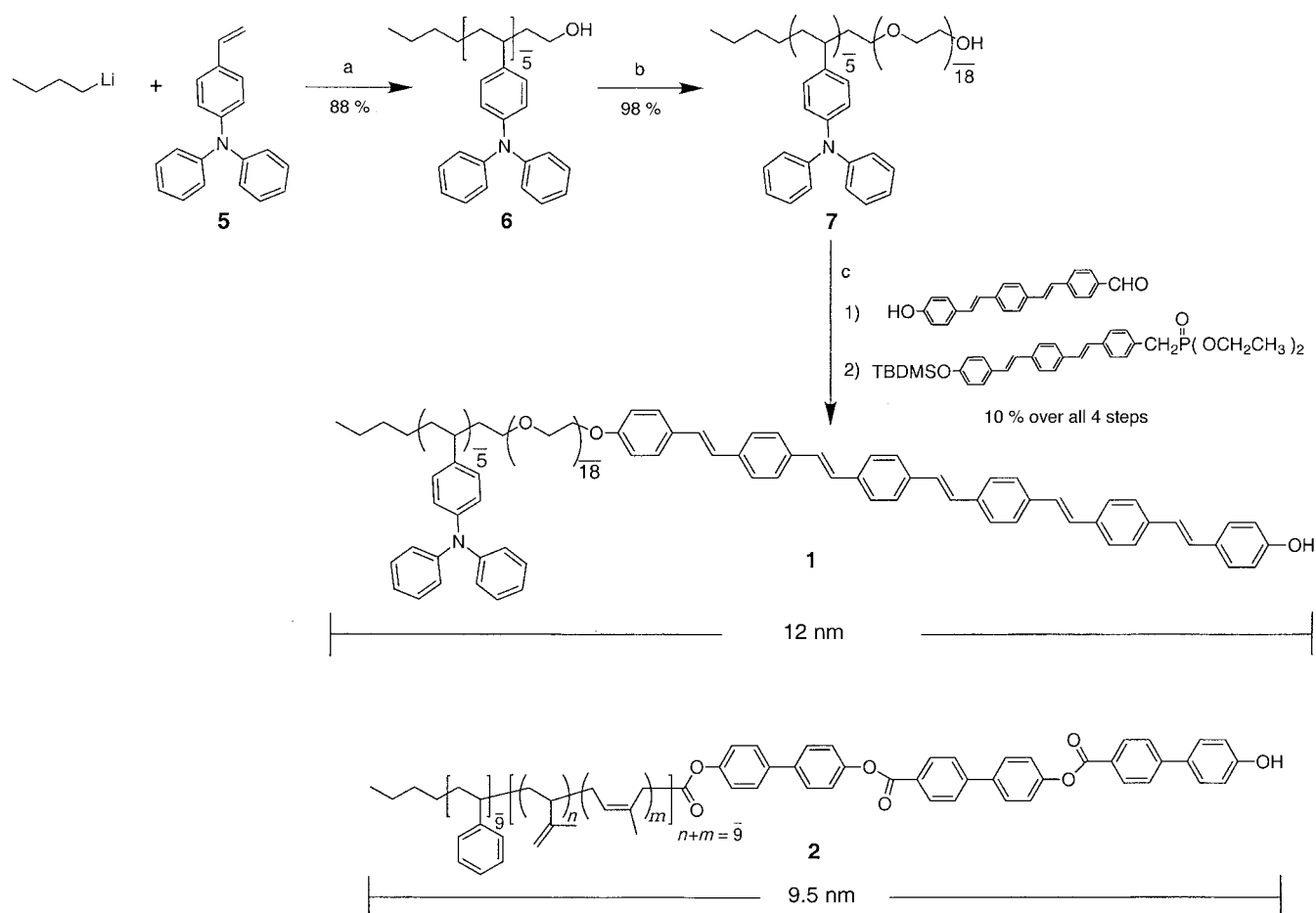


Scheme 1. Reagents: a) $[\text{Pd}_2(\text{dba})_3]$ (2 mol %), dppf (3 mol %), sodium *tert*-butoxide, dry toluene, 70 °C, 8 h; b) DIBALH, THF, –78 to –20 °C, 7 h; c) methyltriphenylphosphonium bromide, LDA, THF, 0 °C to RT. dba = dibenzylideneacetone, DIBALH = diisobutylaluminum hydride, LDA = lithium diisopropylamide, RT = room temperature.

Typical anionic living polymerization conditions followed by quenching of the reaction with ethylene oxide as gas yielded the oligomer **6** of TPA in 88 % yield (Scheme 2).^[9]

[*] Prof. S. I. Stupp, G. N. Tew, M. U. Pralle
Departments of Materials Science and Engineering and Chemistry
Northwestern University
2225 North Campus Drive, Evanston, IL 60208 (USA)
E-mail: s-stupp@nwu.edu
Fax: (+1) 847-491-7820

[**] This work was performed at the University of Illinois at Urbana-Champaign and supported by grants from the Army Research Office (DAAH04-96-1-0450) and the Office of Naval Research (N00014-96-1-0515). G.N.T. wishes to thank the Beckman Institute for Advanced Science and Technology at the University of Illinois for a research assistantship (1997–1998) and the ACS Division of Organic Chemistry for a fellowship (1998–1999).



Scheme 2. Reagents: a) 1. Benzene/THF (10/1), RT, 30 min; 2. ethylene oxide (gas), RT, 30 min; 3. MeOH; b) 1. potassium dihydronaphthylide, THF, RT; 2. ethylene oxide, 45 °C, 24 h; c) 1. methyl sulfonic anhydride, pyridine, CH₂Cl₂, 0 °C, 48 h; 2. Cs₂CO₃, tetrabutylammonium bromide, THF, 70 °C, 48 h; 3. LDA, THF, –78 to –20 °C; 4. 0 °C to RT; 5. tetrabutylammonium fluoride, THF, –78 °C, 4 h (TBDMS = *tert*-butyldimethylsilyl).

Oligomer **6** has a polydispersity index (PDI) of 1.09 by gas-phase chromatography (GPC) and 1.08 by MALDI mass spectrometry. The MALDI mass spectrum of **6** displays a classic Poisson distribution (Figure 1). Other work has been reported on a very different synthetic route to monomer **5**.^[16, 17] Polymerization of ethylene oxide used modified procedures reported by Hillmyer and Bates^[18] with a simpler reaction setup. These polymerization conditions afforded the diblock oligomer **7** (PDI = 1.10 by GPC). The synthesis of the all-*trans* PV rod and its covalent grafting to the coil has been reported previously.^[7]

Polarized optical microscopy (POM) investigations showed **1** to be a thermotropic liquid crystalline material with birefringence from room temperature to 300 °C, where the material becomes isotropic. Small-angle X-ray scattering (SAXS) reflections (Figure 2) indicate a *d*-spacing of 9.2 nm. This spacing is consistent with a monolayer-type packing because the spacing is slightly less than the fully extended length of the molecule. However, a definite assignment of the reflection as the (001) *d*-spacing cannot be made unequivocally in the absence of higher order reflections. Nonetheless several previously characterized triblock systems show *d*-spacings with higher order reflections that confirm the presence of a monolayered material.^[7] These previous systems

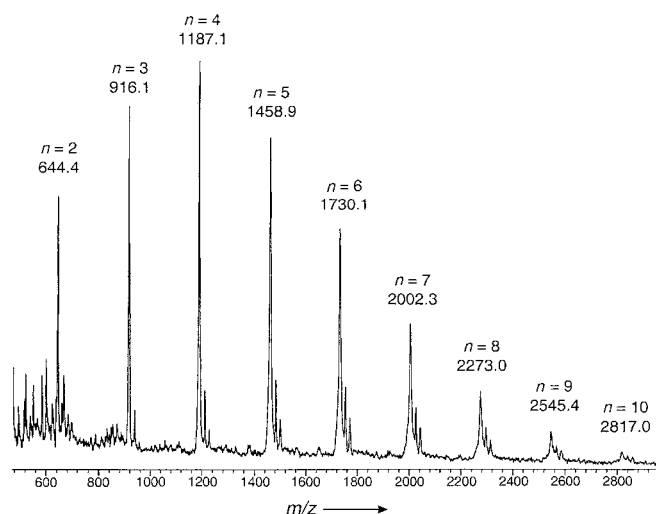


Figure 1. MALDI mass spectrum of **6** showing the peaks associated with different chain lengths, the narrow polydispersity, and the Poisson distribution of the oligomeric segments of TPA.

display similar primary spacings as found for **1**, suggesting this material may also be layered. Furthermore, the electron micrograph discussed below is not consistent with hexagonal or cubic symmetry.

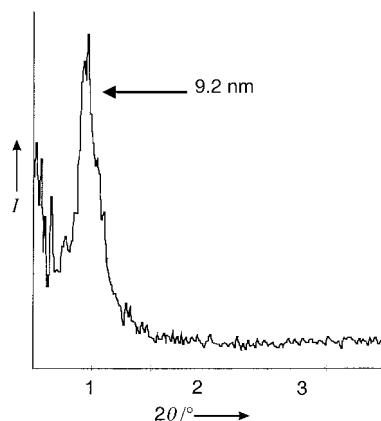


Figure 2. SAXS curve of **1** indicating a layer spacing of 9.2 nm, which suggests monolayer and not bilayer formation.

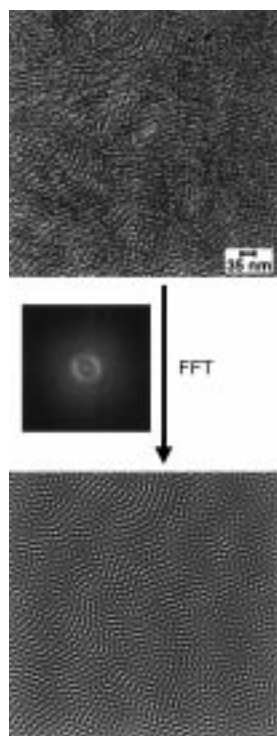


Figure 3. TEM micrograph (top), Fourier filter FFT (middle), and transformed image of **1** (bottom). Micrographs characterize the aggregates as circular with center-to-center distances of 12 nm. The nanostructures are positioned on a pseudo-hexagonal lattice with $a = b = 12$ nm, and an angle of 68° .

When thin films of **1** were characterized by transmission electron microscopy (TEM), we found that indeed nanophase segregation into discrete objects occurs in this particular system. A typical TEM micrograph is shown in Figure 3 along with its Fourier-filtered image, which reveals clearly the dark–light contrast expected in these nanostructured systems. Electron diffraction (ED) indicates this material contains crystalline domains, which is a characteristic of our other self-organized triblock systems. Therefore in the image, contrast between light and dark regions arises from strong diffraction scattering in the rod domains versus weak scattering in the amorphous coils. Upon use of an objective aperture these scattering events were removed from the image, generating the observed contrast. For this reason, the dark areas should contain the rod segments of **1** while the lighter regions must be composed of amorphous domains of coil segments, presumably the TPA and ethylene oxide segments. Figure 3 shows the nanostructures formed by **1** are arranged in an

oblique two-dimensional superlattice with an angle of 68° and dimensions of $a = 12$ nm and $b = 12$ nm. These nanostructures are larger than the nanostructures formed by **2**, as expected based on the fact that molecule **1** is longer than **2**.

Interestingly, the ED pattern in Figure 4 top suggests rod segments in **1** are oriented perpendicular to the plane of the film, and the crystal structure is identical to that found in a

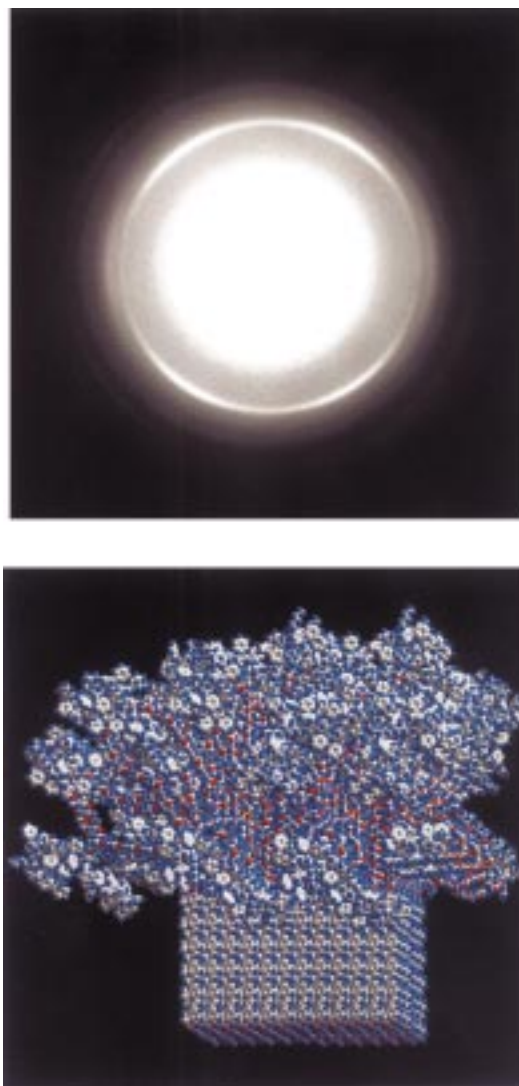


Figure 4. The ED pattern (top) shows films of **1** to contain crystalline domains. The rods crystallize into a unit cell very similar to that of poly(*p*-phenylene vinylene). Based on the ED pattern, TEM image, and SAXS curve, the supramolecular aggregate should be composed of approximately 144 molecules as is shown at the bottom.

previously investigated rodcoil material containing oligostyrene, oligoisoprene, and the same rod segments.^[7] Also, this crystal structure is essentially identical to that observed in poly(*p*-phenylene vinylene) when viewed down the *c* axis, as the rod segments within the nanostructure pack in a herringbone fashion with unit cell dimensions of $a = 7.95$ Å and $b = 5.15$ Å.^[19] However, this is a two-dimensional lattice where *c*-direction order is interrupted by alternating layers of amorphous coil blocks and crystallized rod segments. The ED pattern shows arcs that have been previously observed in rodcoil systems and indicate orientation between objects.^[3, 7] In the ED pattern, reflections corresponding to crystallization of the ethylene oxide coil are not observed, suggesting that both ethylene oxide segments and TPA segments are contained in amorphous domains. The lack of crystallinity in the ethylene oxide segments is probably due to confinement between TPA and rod segments. Figure 4bottom shows a schematic drawing of the supramolecular aggregate.

Figure 5a shows emission spectra from **1** and **6** when the excitation wavelength is 302 nm. This excitation wavelength is λ_{max} for TPA chromophores and is almost transparent for

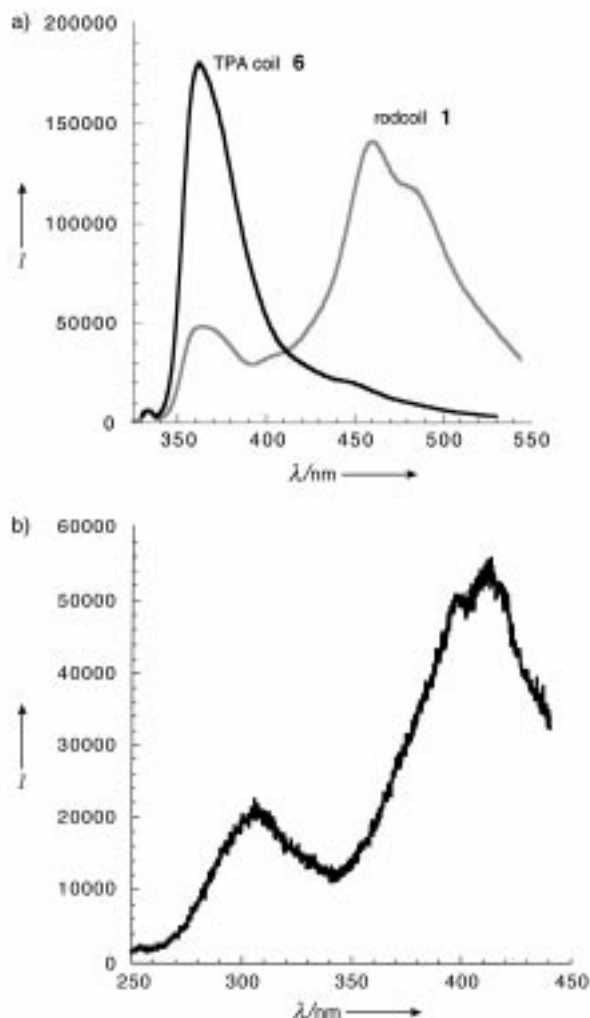


Figure 5. a) Emission spectra from **6** and **1** at the same optical density using 302 nm as the excitation wavelength. The emission spectra suggest energy transfer between the coil and the rod segments. b) An excitation spectrum of **1** with monitoring at 460 nm indicates emission for the coil. This strongly supports energy transfer between coil and rod segments.

structural units in the PV rod segments. The emission curve containing only one peak is from **6** and characterizes the oligo-TPA segments as having an emission with a maximum at 368 nm. Interestingly, the emission of **1** when excited with light at 302 nm shows substantial emission from PV segments. Additional experiments^[20] on quantum efficiency, solvent dielectric measurements, and the excitation scan shown in Figure 5b suggest that energy transfer is occurring between the coil-like TPA and rod-like PV segments of these molecules. Although there is some absorption and emission from rod blocks at 302 nm, the evidence of energy transfer from molecular coil to molecular rod is strong. The observation of energy transfer has been reported within block copolymers;^[21, 22] however, the design of nanostructured systems with luminescent properties is of current interest. An interesting possibility for this system would be the stacking

of the interactive functions into contact as a result of the three-dimensional arrangement of supramolecular nanostructures.

The formation of highly monodisperse and ordered supramolecular nanostructures by design has been demonstrated using the rules of sterically frustrated crystallization. The chemical design of the molecules studied incorporated functions of electronic and photonic interest in their primary sequence. This fact suggests that a broad range of functional chemistries could be used to design nanostructured organic materials.

Experimental Section

SAXS studies were carried out on a Siemens Anton Paar High-Resolution Small Angle Camera equipped with a Hi-Star area detector and Siemens SAXS software mounted on an M18X-HF22 SRA rotating anode generator. Powder diffraction rings were integrated over 360° to yield the diffraction patterns, and the system was calibrated using a silver behenate standard. TEM studies were performed on a Phillips CM 200 TEM operating at 120 keV accelerating voltage.

3: Diphenylamine (4.48 g), 4-bromobenzonitrile (4.38 g), $[\text{Pd}_2(\text{dba})_3]$ (0.44 g), dppf (0.40 g), sodium *tert*-butoxide (3.24 g), and dry toluene (200 mL, ca. 0.1 M based on amine) were heated to 70 °C for 8 h. Upon cooling to room temperature, the reaction mixture was filtered and concentrated by rotatory evaporation. The material was purified by column chromatography ($\text{CH}_2\text{Cl}_2/\text{hexane}$ 40/60) to give **3** as a white solid (5.39 g, 78 % yield). ^1H NMR (500 MHz, CDCl_3): δ = 7.41 (d, J = 9.0 Hz, 2H), 7.33 (t, J = 7.9 Hz, 4H), 7.16 (m, 6H), 6.96 (d, J = 8.8 Hz, 2H).

4: Compound **3** (5.0 g) was dissolved in Et_2O (185 mL) and the solution cooled to –78 °C. Subsequently DIBALH (28 mL, 1.0 M in hexane) was added. The reaction was stirred overnight at –20 °C, and then the mixture was transferred by cannula onto 10 % AcOH/ice. The Et_2O layer that separated was collected. Column chromatography in CH_2Cl_2 gave **4** as a yellow solid (4.83 g, 95 % yield). ^1H NMR (500 MHz, CDCl_3): δ = 9.81 (s, 1H), 7.68 (d, J = 8.8 Hz, 2H), 7.34 (t, J = 8.2 Hz, 4H), 7.17 (m, 6H), 7.01 (d, J = 8.6 Hz, 2H); ^{13}C NMR (125 MHz, CDCl_3 , attached proton test (APT)): δ = 90.5 (CHO), 153.4 (C_{ar}), 146.2 (C_{ar}), 131.4 (C_{ar}), 129.8 (C_{ar}), 129.2 (C_{ar}), 126.4 (C_{ar}), 125.2 (C_{ar}), 119.4 (C_{ar}); FAB-MS: m/z : 273 [M^+].

5: Methyltriphenylphosphonium bromide (7.20 g) was treated with freshly prepared LDA (2 equiv.) in THF (180 mL) at –78 °C. This mixture was allowed to warm to 0 °C, and then a solution of **4** (2.50 g in 30 mL THF) was added by cannula. The reaction mixture was stirred at room temperature overnight after which it was poured into $\text{H}_2\text{O}/\text{Et}_2\text{O}$ and the organic layer was washed with H_2O and saturated aq. NaCl. The organic layer was collected, dried, filtered, and concentrated by rotatory evaporation to give a crude white solid, which was purified by column chromatography ($\text{CH}_2\text{Cl}_2/\text{hexane}$ 1/99, a small amount of toluene helps dissolve the crude solid) to afford **5** as a white solid (2.26 g, 91 % yield). ^1H NMR (500 MHz, CDCl_3): δ = 7.29 (d, J = 8.4 Hz, 2H), 7.25 (m, 4H), 7.09 (d, J = 7.5 Hz, 4H), 7.02 (m, 4H), 6.66 (dd, J = 17.6, 10.6 Hz, 1H), 5.64 (dd, J = 17.6, 0.9 Hz, 1H), 5.16 (dd, J = 10.6, 0.9 Hz, 1H); ^{13}C NMR (125 MHz, CDCl_3 , APT): δ = 47.8 (C_{ar}), 147.7 (C_{ar}), 136.4 (C_{vinyl}), 132.1 (C_{ar}), 129.5 (C_{ar}), 127.3 (C_{ar}), 124.6 (C_{ar}), 123.8 (C_{ar}), 123.1 (C_{ar}), 112.4 (C_{vinyl}); EI-MS: m/z : 271 [M^+].

6: Benzene (100 mL) and THF (15 mL) were placed in a flask, and *n*BuLi (2.11 mL) was added. A solution of **5** (3.40 g) in benzene (20 mL) and THF (7.5 mL) was added by cannula. The reaction mixture was stirred for 30 min and then quenched by bubbling dry ethylene oxide through the solution. The solvent was evaporated by rotatory evaporation, and the crude material was purified by chromatography on silica gel ($\text{CH}_2\text{Cl}_2/\text{hexane}$ 20/80) to provide **6** (3.15 g, 88 % yield). ^1H NMR (500 MHz, CD_2Cl_2): δ = 6.95 (brm, 77H), 3.38 (brm, 2H), 2.24 (brm, 8H), 1.05 (brm, 13H), 0.87 (m, 3H); GPC (254 nm, THF): PDI = 1.09, M_n = 1236; FD-MS: PDI = 1.08, M_n = 1902; MALDI-MS: PDI = 1.14, M_n = 1957.

7: Compound **6** (0.50 g) was dissolved in THF/DMSO (10/1), and potassium dihydronaphthylide was titrated into the reaction mixture until a slight

green color persisted for more than 20 min. Ethylene oxide was condensed to a liquid (0.21 mL) and added to the reaction mixture. The flask was sealed and heated at 45 °C for 8 h. After cooling to room temperature, the THF was removed by rotatory evaporation. Filtration through a plug of silica gel removed DMSO and naphthalene by-products (**7**: 0.61 g, 98 % yield). ¹H NMR (500 MHz, CD₂Cl₂): δ = 6.95 (brm, 73H), 3.57 (brm, 72H), 3.17 (brm, 2H), 2.24 (brm, 8H), 1.05 (brm, 13H), 0.85 (m, 3H); GPC (254 nm, THF): PDI = 1.13, *M_n* = 1489.

1: ¹H NMR (500 MHz, CD₂Cl₂): δ = 6.95 (brm, 120H), 3.57 (brm, 80H), 2.24 (brm, 8H), 1.05 (brm, 13H), 0.85 (m, 3H); GPC (254 nm, THF): PDI = 1.15, *M_n* = 2277.

Received: August 26, 1999 [Z13928]

- [1] J. M. Lehn, *Supramolecular Chemistry*, VCH, New York, **1995**.
- [2] *Comprehensive Supramolecular Chemistry*, Vol. 11 (Eds.: J. L. Atwood, J. E. D. Davies, D. D. MacNicol, F. Vögtle), Pergamon, New York, **1996**.
- [3] S. I. Stupp, V. LeBonheur, K. Walker, L. S. Li, K. Huggins, M. Keser, A. Amstutz, *Science* **1997**, 276, 384–389.
- [4] E. R. Zubarev, M. U. Pralle, L. M. Li, S. I. Stupp, *Science* **1999**, 283, 523–526.
- [5] M. U. Pralle, C. M. Whitaker, P. V. Braun, S. I. Stupp, unpublished results.
- [6] G. N. Tew, L. M. Li, S. I. Stupp, *J. Am. Chem. Soc.* **1998**, 120, 5601–5602.
- [7] G. N. Tew, M. U. Pralle, S. I. Stupp, *J. Am. Chem. Soc.* **1999**, in press.
- [8] *Polymers for Light Wave and Integrated Optics* (Ed.: L. A. Hornak), Marcel Dekker, New York, **1992**.
- [9] M. Morton, *Anionic Polymerization: Principles and Practice*, Academic Press, New York, **1983**.
- [10] J. Lindsey, *Tetrahedron* **1984**, 40, 1433–1456.
- [11] J. F. Hartwig, *Angew. Chem.* **1998**, 110, 2154–2177; *Angew. Chem. Int. Ed.* **1998**, 37, 2047–2067.
- [12] J. P. Wolfe, S. Wagaw, S. L. Buchwald, *J. Am. Chem. Soc.* **1996**, 118, 7215–7216.
- [13] M. Kosugi, M. Kameyama, T. Magita, *Chem. Lett.* **1983**, 927–930.
- [14] S. Thayumanavan, S. Barlow, S. R. Marder, *Chem. Mater.* **1997**, 9, 3231–3235.
- [15] G. N. Tew, L. M. Li, M. U. Pralle, S. I. Stupp, *Abstr. Pap. MRS* (Boston, MA) **1997**, p. J3.35.
- [16] W. J. Feast, R. J. Peace, I. A. Sage, E. L. Wood, *Polym. Bull.* **1999**, 42, 167–174.
- [17] R. G. Compton, M. E. Laing, A. Ledwith, I. Abu-Abdoun, *J. Appl. Electrochem.* **1988**, 18, 431–440.
- [18] M. A. Hillmyer, F. S. Bates, *Macromolecules* **1996**, 29, 6194–7002.
- [19] T. Granier, E. L. Thomas, D. R. Gagnon, F. E. Karasz, R. W. Lenz, *J. Polym. Sci. B* **1986**, 24, 2793–2804.
- [20] The fact that the TPA and PV chromophores both have absorbance at 302 nm makes the interpretation of energy transfer more difficult. To determine if indeed energy transfer is occurring several experiments were performed. The absorption and emission spectra were measured in six different dielectric solvents to rule out electron transfer; the solvents, in order of decreasing dielectric constant, were acetonitrile, tetrahydrofuran, chloroform, diethyl ether, benzene, and cyclohexane. There was no observable shift in λ_{max} for absorption or emission. A series of different concentrations was investigated with UV/Vis spectroscopy to ensure no molecular aggregation was occurring in solution. The concentration was varied from optical density of 0.1 to 1.1 absorbance units. Finally, quantum efficiencies (ϕ) were determined to be $\phi = 0.07$ for **6** and $\phi = 0.04$ for **1**.
- [21] D. M. Watkins, M. A. Fox, *J. Am. Chem. Soc.* **1996**, 118, 4344–4353.
- [22] S. E. Webber, *Chem. Rev.* **1990**, 90, 1469–1482.

Kinetic Footprinting of an RNA-Folding Pathway Using Peroxynitrous Acid**

Steven G. Chaulk and Andrew M. MacMillan*

Complex RNA molecules are at the heart of a number of fundamental biological processes, including translation, tRNA maturation, and RNA splicing.^[1] The unique three-dimensional structures adopted by these molecules determine their activity and in some cases, such as the assembly of the spliceosome, a dynamic series of rearrangements of the RNA structure is required to assemble an active catalytic complex. Considerable progress has been made, using phylogenetic, X-ray, NMR, and chemical probing techniques, towards understanding the two- and three-dimensional structures adopted by large RNAs.^[2–8] The mechanisms and pathways by which large RNAs fold into these structures are obviously of interest, and there is a need for novel approaches to study these processes.

One of the most powerful techniques for probing nucleic acid structure is chemical footprinting. Diffusible hydroxyl radicals produced from Fe-ethylenediaminetetraacetate (EDTA) or Cu-phenanthroline complexes effect cleavage of the phosphodiester backbone of both DNA and RNA; cleavage of radio-labeled molecules can be easily analyzed on high-resolution polyacrylamide gels.^[9, 10] Protection against such cleavage through binding of a protein or formation of a higher order structure is detected as an area of reduced cleavage or footprint. These commonly used footprinting techniques may be regarded as *thermodynamic* since the radicals are typically generated over a 10–60 minute time period and thus are useful for examining a system at equilibrium. Elegant *kinetic* footprinting studies were performed by Chance, Brenowitz, Woodson, and co-workers to elucidate the folding pathway of the Group I ribozyme—radicals were produced on a 50–100 ms timescale by synchrotron X-ray irradiation of folding reactions and allowed the visualization of discrete intermediates on the folding pathway.^[11] Our interest in the dynamics of RNA structure has prompted us to explore the application of other readily available chemical footprinting reagents to kinetic studies of RNA folding. Here we describe the first use of such a reagent, peroxynitrous acid, as a tool for examining the folding pathway of a complex RNA: the *Tetrahymena* ribozyme.

Peroxynitrous acid (HOONO) is unstable in aqueous solution, undergoing homolytic cleavage to generate hydroxyl radical and nitrogen dioxide,^[12, 13] and has been employed in

[*] Prof. A. M. MacMillan, S. G. Chaulk
Department of Chemistry
University of Toronto
Toronto, ON, M5S-3H6 (Canada)
Fax: (+1) 416-978-8603
E-mail: amacmill@chem.utoronto.ca

[**] A.M.M. acknowledges support from the Natural Sciences and Engineering Research Council of Canada. The authors are grateful to Vernon Anderson for calling their attention to peroxynitrous acid as a footprinting reagent. We thank Martha Rook and Jamie Williamson for providing plasmid pT7L-21 and we are grateful to Vanita Sood and Rick Collins for helpful discussions.